

Coherence–incoherence crossover in the normal state of iron oxypnictides and importance of Hund's rule coupling

This article has been downloaded from IOPscience. Please scroll down to see the full text article.

2009 New J. Phys. 11 025021

(<http://iopscience.iop.org/1367-2630/11/2/025021>)

View [the table of contents for this issue](#), or go to the [journal homepage](#) for more

Download details:

IP Address: 128.6.229.87

The article was downloaded on 10/08/2010 at 18:59

Please note that [terms and conditions apply](#).

Coherence–incoherence crossover in the normal state of iron oxypnictides and importance of Hund’s rule coupling

K Haule¹ and G Kotliar

Department of Physics, Rutgers University, Piscataway, NJ 08854, USA

E-mail: haule@physics.rutgers.edu

New Journal of Physics **11** (2009) 025021 (13pp)

Received 16 December 2008

Published 27 February 2009

Online at <http://www.njp.org/>

doi:10.1088/1367-2630/11/2/025021

Abstract. A new class of high-temperature superconductors based on iron and arsenic was recently discovered (Kamihara *et al* 2008 *J. Am. Chem. Soc.* **130** 3296), with the superconducting transition temperature as high as 55 K (Ren *et al* 2008 *Chin. Phys. Lett.* **25** 2215). Here we show, using microscopic theory, that the normal state of the iron pnictides at high temperatures is highly anomalous, displaying a very enhanced magnetic susceptibility and a linear temperature dependence of the resistivity. Below a coherence scale T^* , the resistivity sharply drops and susceptibility crosses over to Pauli-like temperature dependence. Remarkably, the coherence–incoherence crossover temperature is a very strong function of the strength of Hund’s rule coupling J_{Hund} . On the basis of the normal state properties, we estimate J_{Hund} to be ~ 0.35 eV. In the atomic limit, this value of J_{Hund} leads to the critical ratio of the exchange constants $J_1/J_2 \sim 2$. While normal state incoherence is common to all strongly correlated superconductors, the mechanism for emergence of the incoherent state in iron oxypnictides is unique due to its multiorbital electronic structure.

The unusually high superconducting critical temperatures in iron oxypnictides together with unusual normal state properties, which do not fit within the standard framework of the Fermi liquid theory of solids, place the iron pnictides in the broad category of strongly correlated superconductors, such as κ organics, cerium and plutonium-based heavy fermions, and cuprate high-temperature superconductors. In all these materials, superconductivity emerges in close

¹ Author to whom any correspondence should be addressed.

proximity to an incoherent state with unconventional spin dynamics, which cannot be described in terms of weakly interacting quasiparticles. Describing the normal state of these materials is one of the great challenges in condensed matter theory and has resulted in numerous controversies in the context of the cuprates.

Iron pnictides show very high resistivity and very large uniform susceptibility in the normal state [1]. Superconductivity emerges from a state of matter with highly enhanced Pauli-like type of susceptibility [3]. As a function of F⁻ doping, the susceptibility peaks at about 5% doping, reaching a value 25 times higher than the Pauli susceptibility given by local density approximation (LDA) [3, 4]. In the parent compound, the resistivity exhibits a peak at 150 K [1] followed by a sharp drop, which is due to a structural transition from tetragonal (space group P4/nmm) to orthorhombic structure (space group Cmma) [3, 7] followed by a spin density wave transition [5, 6] at lower temperatures. Only a 5% doping completely suppresses the specific heat anomaly [8], while resistivity still shows a very steep drop below a characteristic temperature T^* [8, 9]. While there are suggestions that the drop in resistivity is due to the opening of a pseudogap and proximity to a quantum critical point in the samarium compound [9], other measurements in the lanthanum compound seem to suggest less exotic and more Fermi liquid-like resistivity at the 10% doping level [10, 11]. Here, we will show that the steep drop in resistivity in doped compounds can be understood on the basis of incoherence–coherence crossover, which is naturally accompanied by gradual screening of the magnetic moments, leading to enhanced magnetic susceptibility and crossover from Currie–Weiss to Pauli-type susceptibility.

Theoretically, electron–phonon coupling is not sufficient for explaining superconductivity in $\text{LaO}_{1-x}\text{F}_x\text{FeAs}$ [12, 13], and spin and orbital fluctuations need to be considered. The weak coupling approach based on random phase approximation (RPA) has been carried out by several groups for a simplified two-band model containing two orbitals, d_{xz} and d_{yz} [14]–[16]. The nature of the superconducting state and the pairing symmetry is apparently very sensitive to the parameters of the model, and therefore it is desirable to reliably determine the parameters of a microscopic Hamiltonian, which is the purpose of this paper.

The electronic structure of the $\text{LaO}_{1-x}\text{F}_x\text{FeAs}$ compound was studied by the density functional theory (DFT) [4] and the dynamical mean field theory (DMFT) [12]. DFT calculations show that this material has a well-separated set of bands with mostly d character in the interval between -2 and 2 eV around the Fermi level [12]. The parent compound has five Fermi surface sheets [4], two electron cylinders, centered around the zone edge (M–A line), and three hole pockets around the zone center (Γ –Z line). Upon doping with electrons, the hole-like pocket quickly disappears. The nesting wave vector between the hole and electron pocket promotes the spin density wave instability, which was actually observed in experiment [6]. Notice, however, that the Bragg peak in neutron experiments remains commensurate and does not change with doping, pointing to the inadequacy of the weak coupling spin density wave scenario.

Figure 1 sketches the crystal field levels, as obtained by LDA, when the localized Wannier orbitals are constructed for Fe-3d states. Notice that the tetragonal splittings are comparable with the t_{2g} – e_g splittings, leaving only two degenerate orbitals, i.e. xz and yz . Notice, however, that the bandwidth of these orbitals, as shown in figure 3 of [12], is of the order of 3 eV, which is one order of magnitude larger than the crystal field splittings.

A naive atomic picture suggests a large magnetic moment on the Fe atom ($S = 2$), and consequently almost classical moments, which cannot condense by Cooper pairing, but would

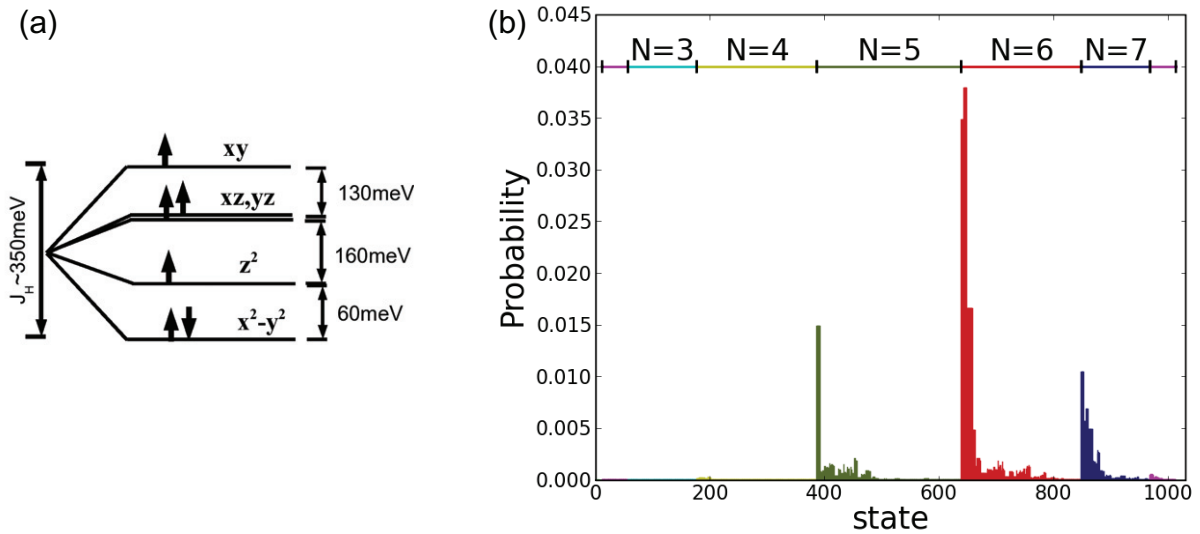


Figure 1. (a) Sketch of the orbital levels in the downfolded LDA Hamiltonian for LaOFeAs, keeping five d-orbitals (see appendix). The levels are obtained by $h_\alpha = \sum_{\mathbf{k}} H_{\mathbf{k},\alpha\alpha}^{\text{LDA}}$, where α is the orbital index. Hund's coupling in this compound becomes relevant when its strength is comparable to the total splitting $J \sim 350$ meV. The coordinate system is chosen such that the x - and y -axes point from an Fe atom toward its nearest neighbor Fe atoms. (b) Probability for each iron 3d atomic state in DMFT calculation for LaOFeAs at $T = 116$ K and $J_{\text{Hund}} = 0.4$ eV. There are 1024 atomic states in the Fe-3d shell. Within the sector with constant occupancy, states are sorted by increasing atomic energy.

rather order magnetically, just like they do in pure iron. Due to degeneracy of xz and yz orbitals, even an infinitesimal Hund's rule coupling would therefore lead to a spin state of at least $S = 1$.

Dynamical mean field studies [12] showed that the correlations in the parent compound are strong enough to make this material a bad metal with a large electronic scattering rate at and below room temperature, as seen in the momentum resolved photoemission spectra and the absence of a Drude peak in the optical conductivity. However, it was argued in [12] that the correlations are *not* strong enough to open the Mott gap in the parent compound, in contrast to the hole doped cuprates, which are known to be doped Mott insulators. The DMFT study determined LaOFeAs to be a strongly correlated metal, which is not well described by either atomic physics or band theory. Furthermore, it was shown that all the five iron d orbitals have appreciable one-particle density of states within 0.5 eV of the Fermi level, and therefore a realistic minimal model for these materials should contain all five d iron orbitals.

In this paper, we use the LDA + DMFT method [17] in combination with the continuous time quantum Monte Carlo method [18] to investigate the transport and thermodynamic properties of the 10% doped $\text{LaO}_{1-x}\text{F}_x\text{FeAs}$ compound. More details of the method are given in [12, 17].

Our goal is to understand why a material with high orbital degeneracy, which naively would have been expected to be an excellent metal², exhibits strong correlation effects and

² Technically, the critical value of the Hubbard U , which is needed to obtain an insulating state (U_{c2}) in an $SU(N)$ symmetric model, is known to scale linearly with orbital degeneracy as N . For this reason, Shorikov *et al* [20], who ignored Hund's rule coupling, concluded that these materials are non-correlated metals.

what determines the crossover from the incoherent regime to the coherent Fermi liquid state. We show that Hund's rule coupling J_{Hund} dramatically reduces the coherence scale T^* in these compounds and promotes the highly incoherent metallic state.

In physical terms, correlated quasiparticles are spin $\frac{1}{2}$ objects that have to be built from atomic states, which are dominantly $S = 2$ and 1, in the presence of Hund's rule coupling. As a result, the overlap of the quasiparticle and the bare electronic states is very small.

To understand the nature of the metallic incoherent state, it is useful to study the probability that an electron in this compound is found in any of the atomic states of the iron 3d orbital. This is plotted in the atomic histogram in figure 1 introduced in [18]. Even the most probable atomic states have a probability of only a few per cent; hence a naive atomic limit is qualitatively wrong for this compound. The atomic histogram characterizes the nature of the ground state of the material. To investigate the coherence–incoherence crossover, we need to probe the excitation spectra through the transport and the thermodynamic probes.

We first turn to the magnetic susceptibility, which is the most direct probe of the spin response:

$$\chi = \frac{(g\mu_B)^2 N_A}{k_B} \int_0^\beta d\tau \langle S_z(\tau) S_z(0) \rangle. \quad (1)$$

Here S_z is the spin of the iron atom, $g\mu_B/2$ is the magnetic moment of a free electron, N_A is the Avogadro number and β is the inverse temperature. In the absence of screening (static S_z), susceptibility should follow the Curie–Weiss law $\chi = [(g\mu_B)^2 N_A S(S+1)]/3k_B T$. In the opposite itinerant limit, the spin susceptibility exhibits the Pauli response $\chi = \mu_B^2 N_A D_0$, where D_0 is the density of state at zero frequency. In figure 2(a), we show the local spin susceptibility for a few values of Hund's coupling J_{Hund} in a 10% doped compound.

In the absence of J_{Hund} , the susceptibility obeys the Pauli law, and the mass enhancement due to correlations is negligible. On the other hand, at the large value of $J_{\text{Hund}} = 0.7$ eV, the system remains in the local moment regime down to the lowest temperature we reached (50 K). For some intermediate values of $J_{\text{Hund}} \sim 0.35$ – 0.4 eV, the system evolves from an incoherent metal at high temperature to the coherent Fermi liquid at low temperature.

The metallicity of the compound always leads to screening of the electron magnetic moments, which eventually disappear at sufficiently low temperature and frequencies, but are present at high temperature and high energies. The scale at which the screening of the local moment takes place, however, is a very sensitive function of the strength of Hund's coupling, being very large for $J_{\text{Hund}} = 0$ and unobservably small for $J_{\text{Hund}} = 0.7$ in the temperature range considered. This is one of the main topics of this paper.

To shed light on the coherence–incoherence crossover, we computed the resistivity due to electron–electron interactions, given by

$$\frac{1}{\rho} = \frac{\pi e^2}{V_0 \hbar} \int d\omega \left(-\frac{df}{d\omega} \right) \sum_{\mathbf{k}} \text{Tr}[v_{\mathbf{k}}(\omega) \rho_{\mathbf{k}}(\omega) v_{\mathbf{k}}(\omega) \rho_{\mathbf{k}}(\omega)], \quad (2)$$

where $v_{\mathbf{k}}$ are velocities of the electrons, $\rho_{\mathbf{k}}$ is the spectral density of the electrons and V_0 is the volume of the unit cell. The resistivity in figure 2(b) demonstrates the crossover even more clearly. The resistivity is approximately linear with a modest slope above the coherence crossover temperature, and it exhibits a steep drop at about the coherence temperature. It is important to stress that the drop in resistivity here is not due to proximity to a quantum critical point [9] or proximity to a spin density wave [5], but because the electrons, being rather

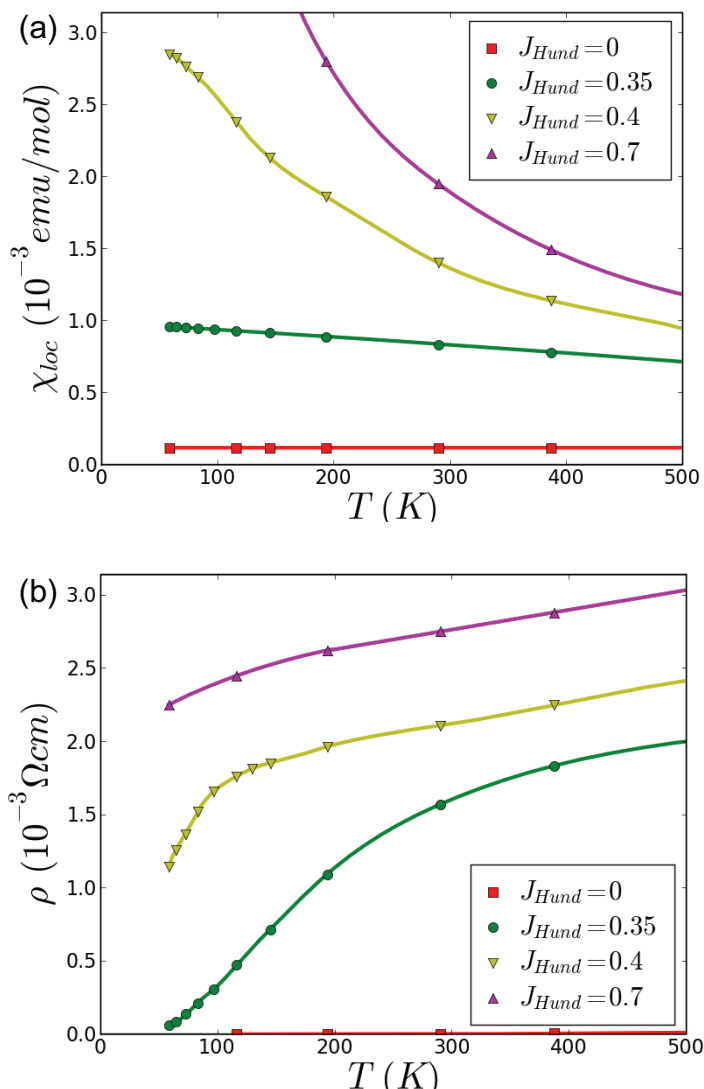


Figure 2. (a) The local susceptibility versus temperature for a few different Hund's coupling strengths. (b) Resistivity versus temperature for the same Hund's coupling strengths.

localized at high temperature, start to form coherent quasiparticle bands with the underlying Fermi surface.

In most compounds, the strength of the correlations is controlled by the ratio of the diagonal on-site Coulomb interaction U to the bandwidth, while Hund's coupling usually plays a sub-leading role. We find that in this compound, a crucial role is played by Hund's coupling. This point was first noticed in the context of a two-band Hubbard model calculation at half-filling [19], and it was shown that the coherence scale is exponentially suppressed when Hund's coupling is taken into account. Moreover, it was emphasized that the non-rotationally invariant Hund's coupling, usually assumed in combination with traditional quantum Monte Carlo methods [20], can lead to qualitatively and quantitatively wrong results. Indeed, we have found that the absence of the rotational invariant Hund's coupling leads to a first-order phase

transition as a function of J_{Hund} , between a Fermi liquid state and a non-Fermi liquid state at zero temperature. On the other hand, the rotational invariance of the Coulomb interaction recovers Fermi liquid at zero temperature, although the coherence scale can become very small, as seen in figure 2(b) for $J_{\text{Hund}} = 0.7$.

It is interesting to note that the atomic J_{Hund} in iron is ~ 1.2 eV. In many materials with correlated f orbitals, the screening of J_{Hund} in a solid is well accounted for by 20% reduction from its atomic value. In the LaOFeAs compound, only 30% of the atomic Hund's coupling gives the best agreement with experiment for resistivity and susceptibility.

To elucidate the sensitivity of mass enhancement with varying of Hund's coupling, we show low-temperature specific heat in figure 3. For small values of J_{Hund} , we find the specific heat value to be very close to the LDA prediction $\gamma \sim 6 \text{ mJ mol}^{-1} \text{ K}^{-2}$. For achieving $J_{\text{Hund}} = 0.35$ eV, a value that gives resistivity in very good agreement with experiments, it is required that the specific heat be enhanced by a factor of 5–30 $\text{mJ mol}^{-1} \text{ K}^{-2}$. This is a large enhancement and should be easy to measure in future experiments, and is a key prediction of the theory. This would be a strong test that a local theory, like the one described in this paper, correctly predicts the physical properties of this material, since it would allow us to differentiate it from paramagnon or itinerant spin density wave theories, where the enhancement of the static susceptibility is much larger than the enhancement of the specific heat. At this point, reliable data on the normal-state specific heat of the doped compound are not available down to sufficiently low temperatures to reliably extract the coefficient γ . It would be interesting to measure it in the slightly doped compound (5%), where the superconducting temperature is low enough and susceptibility shows the strongest enhancement.

The full computation of the momentum-dependent spin response within LDA + DMFT is still a formidable task. However, one can gain insights into the momentum dependence of χ by making a simplifying assumption that, near the Mott transition, $\chi(\mathbf{q})^{-1} = a + J_{\mathbf{q}}$, where $J_{\mathbf{q}}$ is the Fourier transform of the exchange constants and a is a local but frequency-dependent object.

We computed the first neighbor J_1 and next-nearest neighbor J_2 exchange constants as a function of Hund's coupling. For this purpose, we first constructed the Wannier orbitals from iron 3d bands (see appendix), we exactly diagonalized the iron atom and we performed the second-order perturbation theory, with respect to iron–iron hopping. This perturbation is carried out around the atomic ground state of the $S = 2$ and 1 sector.

Figure 3(b) shows the exchange constants as a function of Hund's rule coupling. This provides complementary information to the exchange constants computed around the band limit, which were recently determined by LDA [21]–[23] and are typically larger in magnitude than those obtained here. The exchange constants are supportive of the actual ordering in the parent compound, determined recently by the neutron scattering experiment [7], if $J_2 > J_1/2$. For a reasonable Hund's coupling, both $S = 1$ and 2 ground states respect this inequality. If we select the $S = 1$ state for the ground state, the next-nearest J_2 is much bigger than J_1 . For the actual ground state of the atom ($S = 2$) and realistic $J_{\text{Hund}} \sim 0.35$, the value of J_2 is close to $J_2 \geq J_1/2$. It is interesting to note that according to a well-known result [25], this particular choice of exchange constants results in large magnetic fluctuations due to frustration. At temperatures above the spin density wave transition, there can also be a second-order Ising phase transition, at which the two sublattice magnetizations of the two interpenetrating Neel sublattices lock together. According to [25], the Ising transition would occur around $T_c \sim J_2 S^2 \sim 200$ K.

The large value of the next-nearest neighbor exchange constant demonstrates that even in the atomic limit, the system is highly frustrated, as pointed out in [21, 24], which gives us more

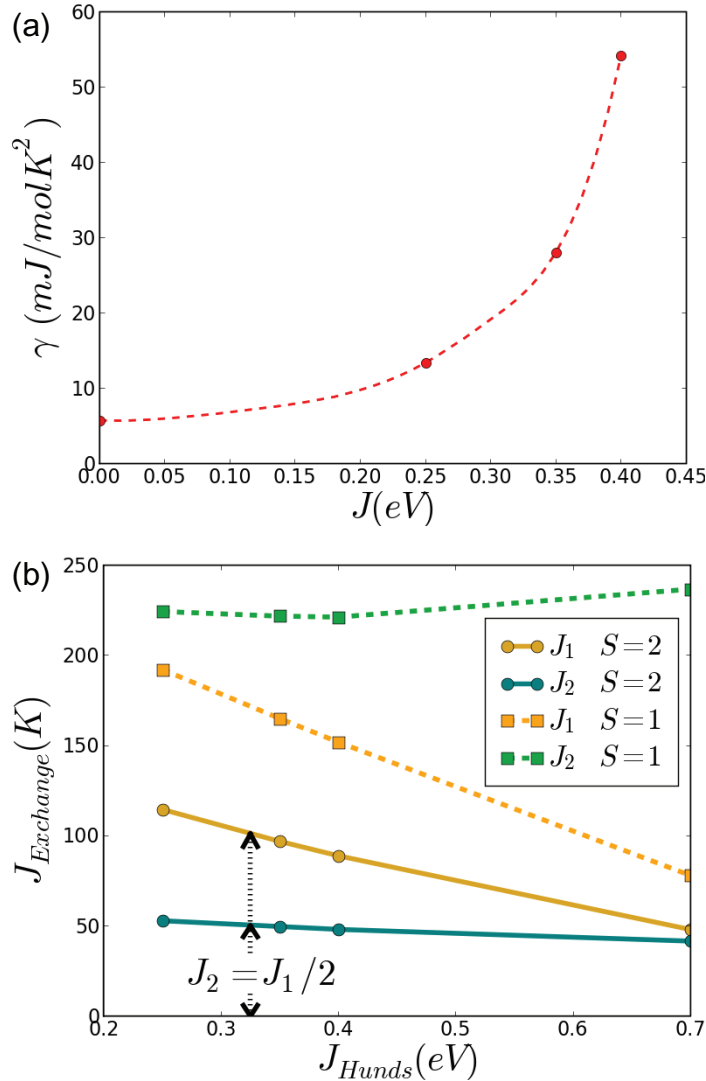


Figure 3. (a) Low-temperature Fermi liquid specific heat coefficient γ versus Hund's coupling strength. The effective mass is exponentially enhanced by the Hund's coupling. The coherence scale is consequentially exponentially suppressed by Hund's coupling. (b) Exchange constants, as obtained from the second-order perturbation theory around the atomic limit, considering either $S=2$, $N=6$ or $S=1$, $N=6$ for the ground state. Positive values for the exchange constants correspond to antiferromagnetic couplings. The rest of the exchange constants are small, for example, $J_3 \sim 1.8$ K and $J_z \sim 0.2$ K.

confidence that the single-site DMFT description, employed in this paper, is adequate, and the momentum-dependent self-energy, as obtained by the cluster extensions of DMFT [17], will not qualitatively change the physics.

From the above provided evidence, the $\text{LaO}_{1-x}\text{F}_x\text{FeAs}$ system fits nicely within the general rubric of strongly correlated superconductivity. The hallmark of this phenomenon is the appearance of an incoherent normal state, above T_c . In the classic Bardeen–Cooper–Schrieffer

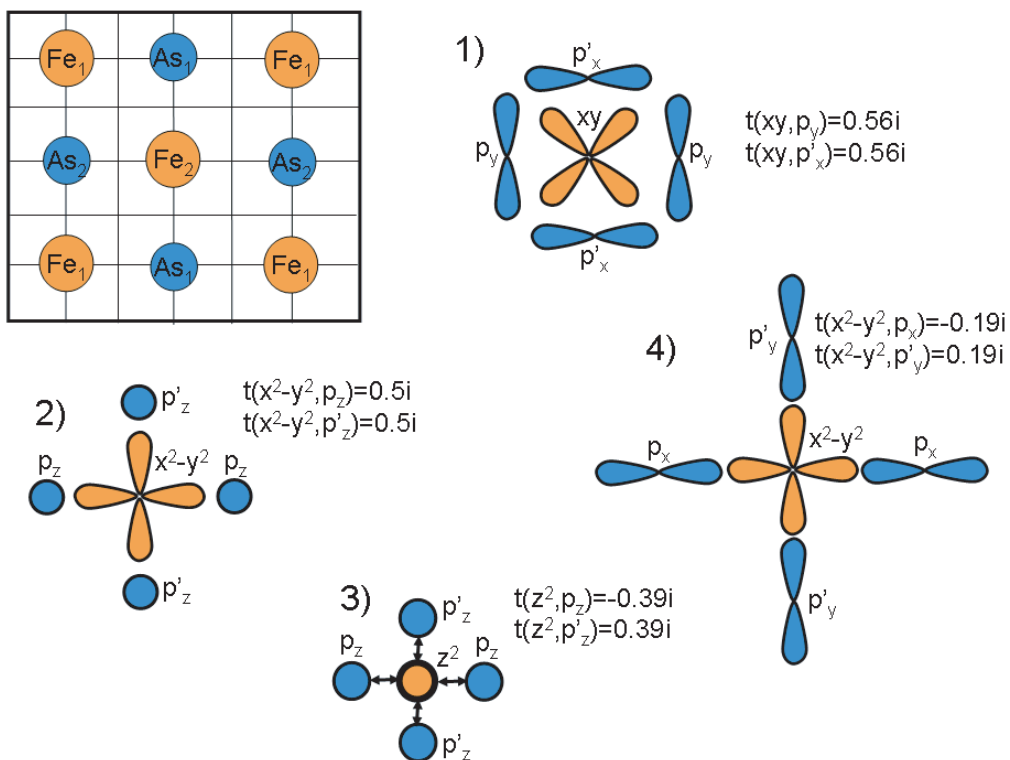


Figure A.1. Top left panel: choice of the unit cell in the Fe–As plane. As_1 lies above the Fe plane and As_2 below it. (1)–(4) Sketch of some of the largest hoppings and their values.

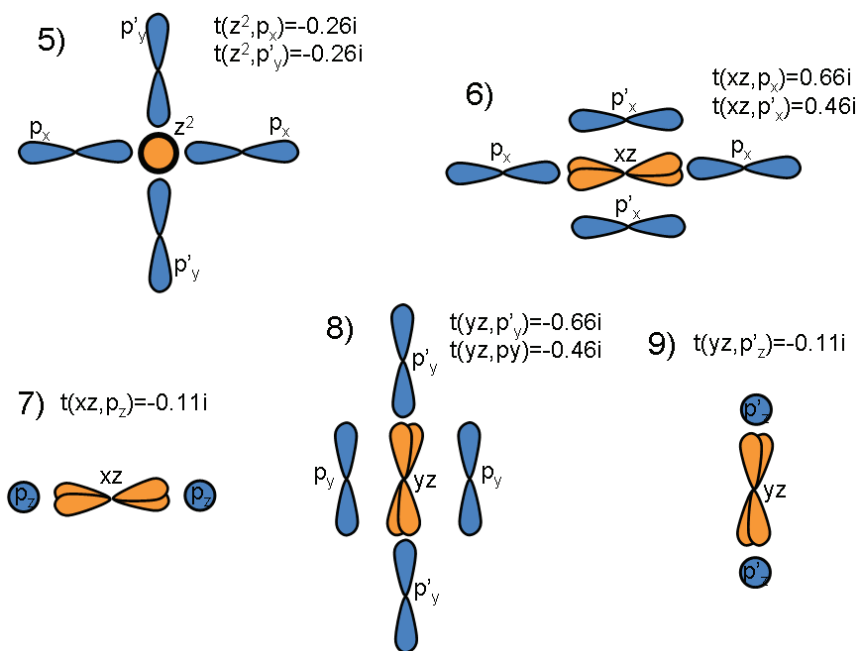


Figure A.2. Sketch of a few more relevant Fe–As hoppings.

Table A.1. On-site energies for both LaFeAsO and LaFePO in the model with both Fe-d and As-p orbitals.

E —on-site	LaFeAsO	LaFePO
$E[x^2 - y^2]$	-0.510	-0.654
$E[yz]$	-0.535	-0.656
$E[z^2]$	-0.564	-0.635
$E[xy]$	-0.650	-0.692
$E[p_z]$	-2.144	-1.990
$E[p_x]$	-2.440	-2.358

Table A.2. The few largest hopping matrix elements in the model of Fe-d and As-p orbitals. Each Fe atom is surrounded by two inequivalent As atoms. The two different As orbitals are sketched in figures A.1 and A.2 and are denoted by p and p'.

Hopping	Figure	LaFeAsO	LaFePO
$xy-p_y$	(1)	0.56*i	0.64*i
$xy-p'_x$	(1)	0.56*i	0.64*i
x^2-p_z	(2)	0.5*i	0.58*i
$x^2-p'_z$	(2)	0.5*i	0.58*i
x^2, p_x	(4)	-0.19*i	-0.33*i
x^2, p'_y	(4)	0.19*i	0.33*i
z^2, p_z	(3)	-0.39*i	-0.45*i
z^2, p'_z	(3)	0.39*i	-0.45*i
z^2, p_x	(5)	-0.26*i	-0.22*i
z^2, p'_y	(5)	-0.26*i	-0.22*i
xz, p_x	(6)	0.66*i	0.76*i
xz, p'_x	(6)	0.46*i	0.51*i
xz, p_z	(7)	-0.11*i	0.0
yz, p_y	(8)	-0.46*i	-0.51*i
yz, p'_y	(8)	-0.66*i	-0.77*i
yz, p'_z	(9)	-0.11*i	0.0

theory of superconductivity, the effective Fermi energy is much larger than the pairing interaction, resulting in small critical temperatures. Strong correlations play the role of reducing the kinetic energy, allowing the pairing interactions to lead to appreciable critical temperatures [26].

While these are common themes shared by all the high- T_c materials, the mechanisms by which different systems manage to renormalize down their kinetic energies, and the details of the competing states that appear as a result, are different in different classes of materials.

Hole doped cuprate superconductors can be modeled as single-band materials, with Coulomb correlation slightly above the Mott transition (in DMFT terminology the effective U , which arises from the charge transfer energy, is above U_{c2}), and indeed maximal T_c is achieved when U is in the vicinity of critical U_{c2} .

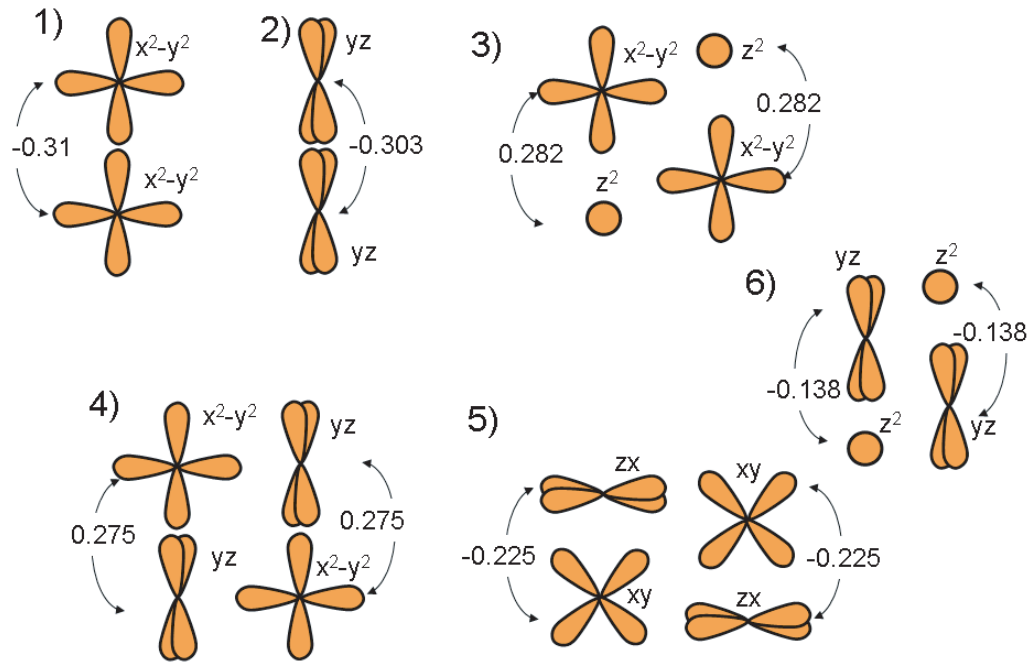


Figure A.3. The sketch of the largest Fe–Fe hoppings in the effective five-band Hubbard model of irons only.

We have argued in our earlier publication [12] that the LaOFeAs is an intrinsically multiorbital system, which is slightly below U_{c2} . The mechanism that is responsible for the incoherence of the normal state and the renormalization of the kinetic energy is Hund's rule J_{Hund} , which we estimate here to be $J_{\text{Hund}} = 0.35\text{--}0.4\text{ eV}$. Competing states in this material are magnetic states, which have been predicted in [5] and since observed by neutron scattering experiments [3, 6, 7].

The incoherent normal states are then eliminated by either a magnetic or a superconducting state, and the study of the competition between these mechanisms in the multiorbital framework deserves further attention.

Appendix. The tight-binding Hamiltonian for the Fe–As planes

The Fe–As planes in LaFeAsO can be described by a tight-binding Hamiltonian containing Fe and As atoms, with two Fe and two As atoms per unit cell (see figure A.1 for a drawing of the unit cell containing Fe_1 , Fe_2 , As_1 and As_2). We obtained the tight-binding parameterization by downfolding the LDA first-principles results, which are expressed in a well-localized muffin tin orbital (MTO) base. The localized nature of the MTO base makes the projection of the Kohn–Sham orbitals to a localized orbital basis set simple and the downfolding procedure more constrained and well defined.

The few largest hoppings are sketched in figures A.1 and A.2. All energies and hoppings are in units of electronvolts. The on-site energies of all orbitals are tabulated in table A.1 and

Table A.3. Continued from table A.2, a few more large hopping matrix elements of the Fe-d and As-p model.

Hopping	LaFeAsO	LaFePO
p_z, p'_z	0.29	0.27
p_x, p'_x	0.16	0.21
p_y, p'_y	0.16	0.21
p_x, p'_z	-0.25	-0.27
p_y, p'_z	0.25	0.27
p_z, p'_x	-0.25	-0.27
p_z, p'_y	0.25	0.27
p_x, p'_y	-0.15	-0.18
p_y, p'_x	-0.15	-0.18
xy, xy'	-0.30	-0.35
$xy, z^{2'}$	0.21	0.24
z^2, xy'	0.21	0.24
$x^2, x^{2'}$	0.19	0.18
yz, xz'	0.15	0.16
xz, yz'	0.15	0.16
$yz, x^{2'}$	0.09	0.12
$xz, x^{2'}$	0.09	0.12
x^2, yz'	0.09	0.12
x^2, xz'	0.09	0.12
$z^2, z^{2'}$	-0.07	-0.06
yz, yz'	0.06	0.07
yz, xy'	0.06	0.07
xz, xz'	0.06	0.07
xz, xy'	-0.06	-0.07
xy, yz'	0.06	0.07
xy, xz'	-0.06	-0.07
$yz, z^{2'}$	-0.02	-0.02
$xz, z^{2'}$	0.02	0.02
z^2, yz'	-0.02	-0.02
z^2, xz'	0.02	0.02

most of the hoppings are tabulated in tables A.2 and A.3. Note that orbitals are expressed in the coordinate system of the four-atom unit cell, shown in figure A.1. The complete set of tight-binding hoppings is available to download³. For comparison we also include the hoppings for a closely related compound, LaFePO, which shows considerably less correlation effects due to somewhat larger crystal field splittings, which renormalize down the effective Hund's coupling.

Further downfolding to the five-band model of Fe is possible. The on-site energies and the few largest hoppings of the corresponding multiorbital Hubbard model are tabulated in

³ The full Hamiltonian for five-band Fe model and eight-band Fe-As model can be downloaded from: <http://www.physics.rutgers.edu/~haule/FeAs/>

Table A.4. The on-site energies and the most important hoppings in the five-band model of Fe-d orbitals only.

Hopping	Figure	LaFeAsO	LaFePO
$E[xy]$		0.096	0.244
$E[yz]$		-0.034	-0.054
$E[z^2]$		-0.189	-0.201
$E[x^2]$		-0.251	-0.162
$x^2, x^{2'}$	(1)	-0.310	-0.343
yz, yz'	(2)	-0.303	-0.356
$x^2, z^{2'}$	(3)	0.282	0.310
$z^2, x^{2'}$	(3)	0.282	0.310
x^2, yz'	(4)	0.275	0.356
$yz, x^{2'}$	(4)	0.275	0.356
zx, xy'	(5)	-0.225	-0.269
xy, zx'	(5)	-0.225	-0.269
$yz, z^{2'}$	(6)	-0.138	-0.104
z^2, yz'	(6)	-0.138	-0.104
zx, zx'		-0.010	-0.035
xy, xy'		-0.086	-0.175
$z^2, z^{2'}$		0.036	0.088
$zx, z^{2'}$		0.004	0.003
z^2, zx'		0.004	0.003
$zx, x^{2'}$		-0.003	0.006
x^2, zx'		0.003	-0.006

table A.4. A sketch of the most relevant hoppings is shown in figure A.3. Note that the coordinate system here is chosen differently from above. Here we use the 45° rotated coordinate system, which corresponds to the usual square lattice of irons.

References

- [1] Kamihara Y, Watanabe T, Hirano M and Hosono H 2008 Iron-based layered superconductor $\text{La}[\text{O}_{1-x}\text{F}_x]\text{FeAs}$ ($x = 0.05\text{--}0.12$) with $T_c = 26\text{ K}$ *J. Am. Chem. Soc.* **130** 3296
- [2] Ren Z-A *et al* 2008 Superconductivity at 55 K in iron-based F-doped layered quaternary compound $\text{Sm}[\text{O}_{1-x}\text{F}_x]\text{FeAs}$ *Chin. Phys. Lett.* **25** 2215
- [3] Nomura T *et al* 2008 Crystallographic phase transition and high- T_c superconductivity in LaOFeAs:F *Supercond. Sci. Technol.* **21** 125028
- [4] Singh D J and Du M H 2008 $\text{LaFeAsO}_{1-x}\text{F}_x$: a low carrier density superconductor near itinerant magnetism *Phys. Rev. Lett.* **100** 237003
- [5] Dong J *et al* 2008 Competing orders and spin-density-wave instability in $\text{La}(\text{O}_{1-x}\text{F}_x)\text{FeAs}$ *Europhys. Lett.* **83** 27006
- [6] McGuire M A *et al* 2008 Phase transitions in LaFeAsO : structural, magnetic, elastic, and transport properties, heat capacity and Mossbauer spectra *Phys. Rev. B* **78** 094517
- [7] de la Cruz C *et al* 2008 Magnetic order versus superconductivity in the iron-based layered $\text{La}(\text{O}_{1-x}\text{F}_x)\text{FeAs}$ systems *Nature* **453** 899

- [8] Ding L *et al* 2008 Specific heat of iron-based high- T_c superconductor $\text{SmO}_{1-x}\text{F}_x\text{FeAs}$ *Phys. Rev. B* **77** 180510
- [9] Liu R H *et al* 2008 Phase diagram and quantum critical point in newly discovered superconductors: $\text{SmO}_{1-x}\text{F}_x\text{FeAs}$ *Phys. Rev. Lett.* **101** 087001
- [10] Sefat A S *et al* 2008 Electron correlations in the low carrier density $\text{LaFeAsO}_{0.89}\text{F}_{0.11}$ superconductor ($T_c = 28\text{ K}$) *Phys. Rev. B* **77** 174503
- [11] Zhu X *et al* 2008 Upper critical field, Hall effect and magnetoresistance in the iron-based layered superconductor $\text{LaO}_{0.9}\text{F}_{0.1-\delta}\text{FeAs}$ *Supercond. Sci. Technol.* **21** 105001
- [12] Haule K, Shim J H and Kotliar G 2008 Correlated electronic structure of LaOFeAs *Phys. Rev. Lett.* **100** 226402
- [13] Boeri L, Dolgov O V and Golubov A A 2008 Is $\text{LaO}_{1-x}\text{F}_x\text{FeAs}$ an electron–phonon superconductor? *Phys. Rev. Lett.* **101** 026403
- [14] Kuroki K *et al* 2008 Unconventional superconductivity originating from disconnected Fermi surfaces in $\text{LaO}_{1-x}\text{F}_x\text{FeAs}$ *Phys. Rev. Lett.* **101** 087004
- [15] Yao Z-J *et al* 2009 Spin fluctuations, interband coupling, and unconventional pairing in iron-based superconductors *New J. Phys.* **11** 025009
- [16] Qi X-L *et al* 2008 Pairing strengths for a two orbital model of the Fe-pnictides arXiv:0804.4332
- [17] Kotliar G *et al* 2006 Electronic structure calculations with dynamical mean-field theory *Rev. Mod. Phys.* **78** 865
- [18] Haule K 2007 Quantum Monte Carlo impurity solver for cluster DMFT and electronic structure calculations in adjustable base *Phys. Rev. B* **75** 155113
- [19] Pruschke Th and Bulla R 2005 Hund’s coupling and the metal–insulator transition in the two-band Hubbard model *Eur. Phys. J. B* **44** 217
- [20] Shorikov A O *et al* 2008 Coulomb correlation effects in LaOFeAs : LDA + DMFT(QMC) study arXiv:0804.3283v1
- [21] Yildirimar T 2008 Origin of the 150 K anomaly in LaOFeAs ; competing antiferromagnetic superexchange interactions, frustration, and structural phase transition *Phys. Rev. Lett.* **101** 057010
- [22] Ma F *et al* 2008 Antiferromagnetic superexchange interactions in LaOFeAs arXiv:0804.3370
- [23] Yin Z P *et al* 2008 Electron–hole symmetry and magnetic coupling in antiferromagnetic LaOFeAs *Phys. Rev. Lett.* **101** 047001
- [24] Si Q and Abrahams E 2008 Strong correlations and magnetic frustration in the high T_c iron pnictides *Phys. Rev. Lett.* **101** 076401
- [25] Chandra P, Coleman P and Larkin A I 1990 Ising transition in frustrated Heisenberg models *Phys. Rev. Lett.* **64** 88
- [26] Capone M, Fabrizio M, Castellani C and Tosatti E 2002 Strongly correlated superconductivity *Science* **296** 2364